Simulation of quantum random walks using the interference of a classical field

H. Jeong, M. Paternostro, and M. S. Kim
School of Mathematics and Physics, The Queen's University, Belfast BT7 1NN, United Kingdom
(Received 10 May 2003; published 16 January 2004)

We suggest a theoretical scheme for the simulation of quantum random walks on a line using beam splitters, phase shifters, and photodetectors. Our model enables us to simulate a quantum random walk using of the wave nature of classical light fields. Furthermore, the proposed setup allows the analysis of the effects of decoherence. The transition from a pure mean-photon-number distribution to a classical one is studied varying the decoherence parameters.

DOI: 10.1103/PhysRevA.69.012310 PACS number(s): 03.67.Lx, 42.25.Hz

I. INTRODUCTION

Random walks are useful models for physicists to study statistical behaviors of nature such as Brownian motions of free particles [1]. They have also been studied for practical use such asalgorithms in computer science [2] and risk management in finance [3]. Quantum versions of random walks have been recently studied for both fundamental interests and the expectation of building new algorithms for quantum computation [4]. There have been several suggestions for a practical implementation of quantum random walks, using ions in linear traps, optical lattices, and cavity QED [5,6]. Recently, proposals for the implementation of quantum random walks with linear optical elements have been suggested [7,8] and the first search algorithm using quantum random walks has been reported [9]. Quantum random walks typically show very different patterns from the Gaussian distributions for classical random walks, which have some remarkable characteristics such as an exponentially fast hitting time [4]. It has been pointed out that these differences are due to the existence of quantum coherence [5].

In this paper, we suggest a theoretical scheme to simulate quantum random walks on a line using the wave nature of classical light fields. This is related to the fact that the idea of quantum coherence is originally borrowed from the interference of wave mechanics shown in Young's double-slit experiment. In our scheme, it is also possible to simulate decoherence processes modeled using additional random phase-shifters and beam splitters with erratic transmittivity. This analysis is relevant under different points of view. First of all it shows that, increasing the amount of decoherence that affects the system, the distribution of the random walk changes from a totally quantum one to a classical Gaussian distribution. This clarifies the role played by the interference effects in the dynamics of a quantum walker and represents an ulterior proof of the validity of a simulation based on interferometric devices. On the other hand, studying the effects of possible sources of errors in our model, we can single out the causes of certain deviations from the ideality in the patterns resulting from performed experiments.

This paper is organized as follows. In Sec. II, we briefly review coined quantum random walks on a line with their characteristics and we suggest a scheme for the simulation of quantum random walks. We will later show that,with this setup, we can simulate quantum random walks using wave nature of a field. This possibility is neither always obvious nor mentioned in other models. It should be pointed out that a similar scheme of all-optical implementation has been suggested by Zhao *et al.* [7]. Their proposal is entirely based on the quantum coherence of a quantum superposition of two polarization degrees of freedom. On the other hand, our scheme is able to take the wave nature of any input field (classical or nonclassical) to show the same interference pattern. This, with the explanation of the role of the phase shifters in our scheme, is shown in Sec. III. Section IV is devoted to the study of the decoherence effects in our proposal. We show that decoherence on the coin tossing operation and on the quantum walker motion can be simulated and studied by means of our system, thus demonstrating the role of the interference effectsin this simulation. This investigation is useful even from a practical point of view because it singles out and characterizes the effect of a class of errors that could affect a performed experiment.

II. QUANTUM RANDOM WALK WITH LINEAR OPTICAL ELEMENTS

In unidimensional coined random walks, the walker is restricted to move along a line with a number of discrete integer points on it.The walker is supposed to be a classical particle on one of the integer points. A coin tossing determines whether the walker moves left or right for each step. In the quantum version of coined random walks, the classical coin is replaced by a quantum bit whose states $|L\rangle$ and $|R\rangle$ represent the logical values LEFT and RIGHT. The quantum coin can be embodied by an internal degree of freedom of the walker itself [4]. The walker, which is a quantum particle, moves conditioned to the result of the coin tossing operation which is realized by a Hadamard transform [5]. For example, the transformation for one step of the particle from an arbitrary point X is simply

$$|X,R\rangle \rightarrow \frac{1}{\sqrt{2}}(|X+1,R\rangle + |X-1,L\rangle),$$
$$|X,L\rangle \rightarrow \frac{1}{\sqrt{2}}(|X+1,R\rangle - |X-1,L\rangle). \quad (1)$$

After n steps, the state of the system is $|\Psi_n\rangle$. Differently from the classical walks on a line, where the position of the particle is monitored at every step of the process, in the quantum version the walker remains in a superposition of many positions until the final measurement is performed. The probability for the particle being at X_k after n steps is $\mathcal{P}_n(X_k)=|\langle R|\langle X_k|\Psi_n\rangle|^2+|\langle L|\langle X_k|\Psi_n\rangle|^2$. During the quantum random walk process, destructive as well as constructive interference may occur. The quantum correlation between two different positions on a line introduced at the first step may be kept by delaying the measurement step until the final iteration.

The probability distribution to find the particle at a given position is generally dependent on the initial state of the system [5] and exhibits avery structured pattern. This allows only numerical evaluations of its variance. It has been shown that, roughly, the standard deviation σ_{QRW} grows linearly with N and is independent of the initial state of the coin [6]. Thus, the walker in quantum walks explores its possible configurations faster than in classical walks, where the standard deviation grows as $\sqrt{N}$. This motivates the conjecture that algorithms based on quantum random walks could beat their classical versions in terms of the time needed to solve a problem [9].

There have been a few suggestions for experimental implementations of quantum random walks [6]. Recently, it has been shown that quantum random walks can be realized using linear optical elements [7]. In this scheme, polarization beam splitters, half-wave plates, and photodetectors are used. The walker is embodied in a single-photon state and the entire scheme is based on the quantum coherence of two polarization states of the photon. This result is inspiring as a proposal for an all-optical implementation of a quantum random walk, even if it requires a reliable single-photon state source, which is very demanding, and the apparatus is highly sensitive to variations in the photons polarization.

First, we propose a scheme which uses ordinary 50:50 beam splitters, phase shifters, and photodetectors. We formulate quantum random walks with the coin tossing operation embedded in the translation of the walker particle. In our scheme, the polarization degree of freedom does not play a role and, thus, is not considered at all. A single-mode field, including a thermal field, may be used as an input to simulate the distribution of the quantum random walk. In fact, this may be apparent if we recall that Young used a thermal field for his double-slit experiment and showed interference.

Let us consider the experimental setup, composed of 50:50 beam splitters, phase shifters, and photodetectors, shown in Fig. 1. For convenience, we denote the field modes propagating sidewards by s and downwards by d. As the beam splitters used here are polarization insensitive, these modes do not refer to polarization. Here, we consider a single-photon state $|1\rangle_s$ as the initial state of the walker and we show that, in this case, our scheme gives rise to coined quantum random walks on a line. At the first beam splitter $\hat{B}_1(\theta,\phi)$ the input field is mixed with a field mode prepared in a vacuum state [Fig. 1(a)]. The following transformation is realized:

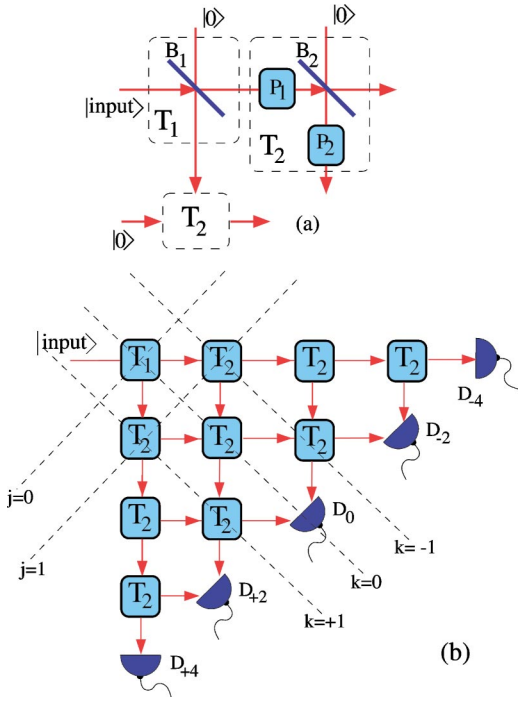

FIG. 1. All-optical setup for the simulation of quantum random walks on a line. (a) Two different kinds of operations are shown: $\hat{T}_1$ is an ordinary beam splitter $\hat{B}_1(\theta,\phi)$ and $\hat{T}_2$ involves the cascade of the phase shifter $\hat{P}_1(\pi/2)$, of a 50:50 beam splitter $\hat{B}_2(\pi/2,\pi)$ and of the phase shifter $\hat{P}_2(-\pi/2)$. (b) Proposed setup, shown up to the fourth dynamic line. Apart from the input state, all the other modes are initially prepared in vacuum states.

$$\hat{B}_1(\theta,\phi)|0,1\rangle_{d,s}=\cos\frac{\theta}{2}|1,0\rangle_{d,s}+e^{i\phi}\sin\frac{\theta}{2}|0,1\rangle_{d,s}, \quad (2)$$

where $\hat{B}_1(\theta,\phi)=\exp\{(\theta/2)(e^{i\phi}\hat{a}_s^\dagger\hat{a}_d-e^{-i\phi}\hat{a}_d^\dagger\hat{a}_s)\}$ is the beam splitter operator and $\hat{a}_{s,d}$ ($\hat{a}_{s,d}^\dagger$) are the annihilation (creation) operators for a sideward and a downward field mode, respectively. We define the transformation in Eq. (2) as $\hat{T}_1$. We introduce the transformation $\hat{T}_2$,

$$|1,0\rangle_{d,s}\rightarrow\frac{1}{\sqrt{2}}(|1,0\rangle+|0,1\rangle)_{d,s}, \quad (3)$$

$$|0,1\rangle_{d,s}\rightarrow\frac{1}{\sqrt{2}}(|1,0\rangle-|0,1\rangle)_{d,s}, \quad (4)$$

which can be realized with a 50:50 beam splitter $\hat{B}_2(\pi/2,\pi)$ and two phase shifters $\hat{P}_1(\pi/2)=e^{i\pi\hat{a}_s^\dagger\hat{a}_s/2}$ and $\hat{P}_2(-\pi/2)=e^{-i\pi\hat{a}_d^\dagger\hat{a}_d/2}$ as shown in Fig. 1(a).

The scheme can simply be illustrated as recursive applications of $\hat{T}_2$ after the initial transformation $\hat{T}_1$, as shown in Fig. 1(b). A dynamic line [7] is represented by a row of aligned optical elements (or photodetectors), labeled j in Fig. 1(b). On the other hand, a node is given by a point represented by k on a dynamic line. For example, the detector

D_{-2} is on the fourth dynamic line and occupies the node $k=-2$. If a photon is incident downward (sideward) on a dynamic line j and node k, we represent its state as $|k,d\rangle_j$ ($|k,s\rangle_j$). The transition from a dynamic line j to $j+1$ by means of the operation $\hat{T}_2$ is synthesized by

$$|k,d\rangle_j \rightarrow \frac{1}{\sqrt{2}}(|k+1,d\rangle+|k-1,s\rangle)_{j+1},$$
$$|k,s\rangle_j \rightarrow \frac{1}{\sqrt{2}}(|k+1,d\rangle-|k-1,s\rangle)_{j+1}. \quad (5)$$

We notice that Eqs. (5) are equivalent to Eqs. (1). Thus, the actions of $\hat{T}_1$ and $\hat{T}_2$ on a single-photon state exactly corresponds to a coined quantum random walk. Any initial coin state, up to an irrelevant global phase, can be prepared by changing θ and φ in $\hat{T}_1$. If $\theta=\pi/2$ and $\phi=-\pi/2$, we get the symmetric probability distribution that corresponds to the initial coin state $(|R\rangle+i|L\rangle)/\sqrt{2}$ in a coined quantum walk [6]. In our model, the difference between quantum and classical walks from a certain step is due to the interference of the walker's paths on the $\hat{T}_2$ processes [11].

III. ANALYSIS WITH DIFFERENT STATES OF THE WALKER

In this section we show that the scheme suggested in Fig. 1 exhibits the same interference pattern at the detectors regardless of the nature of the input state. We first address the case of an input coherent state and, then, we extend the analysis to any field.

A. Coherent states

A coherent state $|\alpha\rangle$ ($\alpha\in\mathbb{C}$) is generally assumed to be the best description of the state of a laser beam. We consider $|\alpha\rangle$ as the input state of the walker. The action of the beam splitter operator on two input coherent states does not lead to any entanglement between the output modes [13]. Assuming $\theta=\pi/2$ and $\phi=-\pi/2$ for the $\hat{T}_1$ process, we can calculate the distribution of the average photon number as a function of the position k on the chosen final dynamic line. For example, for $N=4$ steps, we find the final state

$$|\Phi_4\rangle=\left|\frac{-i\alpha}{4},s\right\rangle_4^{-4}\left|\frac{-i\alpha}{4},d\right\rangle_4^{-2}\left|\frac{1-2i}{4}\alpha,s\right\rangle_4^{-2}\left|\frac{\alpha}{4},d\right\rangle_4^{0}$$
$$\otimes\left|\frac{i\alpha}{4},s\right\rangle_4^{0}\left|\frac{-2-i}{4}\alpha,d\right\rangle_4^{+2}\left|\frac{\alpha}{4},s\right\rangle_4^{+2}\left|\frac{-\alpha}{4},d\right\rangle_4^{+4}, \quad (6)$$

with $|\alpha,s\rangle_j^k$ ($|\alpha,d\rangle_j^k$) indicating a coherent state incident sideward (downward) on a dynamic line j and node k. The average photon-number $\mathcal{N}_p(N,k)$ for node k is $\mathcal{N}_p(4,k)=\mathcal{M}(4,k)\mathcal{N}_{in}(|\alpha\rangle)$, with

$$\mathcal{M}(4,\pm4)=\tfrac{1}{16},\mathcal{M}(4,\pm2)=\tfrac{3}{8},\quad \mathcal{M}(4,0)=\tfrac{1}{8}. \quad (7)$$

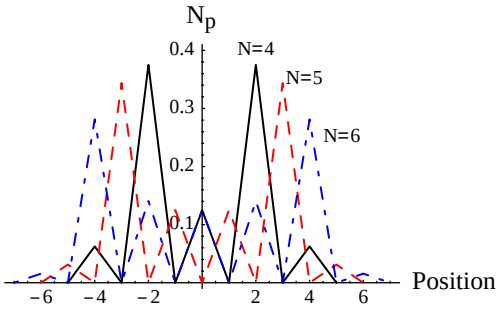

FIG. 2. Average photon-number distribution for an input coherent state $|\alpha=1\rangle$, as a function of the position along the final dynamic line. Three different cases are considered: the solid-line curve is relative to a number of steps $N=4$, the dashed-line represents $N=5$, while the dot-dashed one is for $N=6$. The plots match perfectly the graphs expected for a coined quantum walk on a line. In the general case of $\alpha\neq1$, N_p has to be normalized with respect to $|\alpha|^2$.

Here, $\mathcal{N}_{in}(|\alpha\rangle)=|\alpha|^2$ is the average photon number for the input state $|\alpha\rangle$ and $\mathcal{M}(N,k)$ is the *normalized photon-number distribution* at step N and node k. It characterizes the output photon-number distribution at the detectors. We find that the distribution $\mathcal{M}(4,k)$ for an input coherent state is the same as the one for the single-photon input [6], i.e., the two different inputs result in the same photon-number distribution. The average photon numbers for steps $N=4,5,6$ are shown in Fig. 2. The deviations of a quantum walk from its classical counterpart appears from the fourth step. This is due to the particular values of the parameters in the transformation $\hat{T}_1$: $\theta=\pi/2$ and $\phi=-\pi/2$. Since a coherent-state input results in the same quantum random-walk pattern of the single-photon case for all the steps we have considered, we conjecture that the quantum walk pattern results, even for any initial state for a general number of steps N. In what follows, we prove the validity of this conjecture.

B. General case

With the proposed setup, the quantum walk process can be represented as

$$|\Phi_N\rangle=\hat{U}_{T(j=N)}\ldots\hat{U}_{T(j=1)}\hat{T}_{1(j=0)}|\Phi_0\rangle\equiv\hat{U}_{QW}^N|\Phi_0\rangle,$$

where $|\Phi_0\rangle$ is the input state, N is the number of steps, and $\hat{U}_T$ is an appropriate unitary transformation for each step. For a coherent state, the previous result can be summarized as

$$|\Phi_0\rangle=|\alpha\rangle\xrightarrow{\hat{U}_{QW}^N}|\chi_1\alpha\rangle_1|\chi_2\alpha\rangle_2\ldots|\chi_N\alpha\rangle_{2N}=|\Phi_N\rangle. \quad (8)$$

Equation (6) is an explicit example. The average photon number for mode r ($0\leq r\leq 2N$) is $n_r=|\chi_r|^2|\alpha|^2=|\chi_r|^2\mathcal{N}_{in}(|\alpha\rangle)$, with $r=0$ corresponding to the mode incident on the detector that occupies $j=N$, $k=-N$. It is easy to show that the average photon number for the kth node and

jth step is given by $\mathcal{N}_p(j,k)=n_{j-k}+n_{j-k+1}=(|\chi_{j-k}|^2+|\chi_{j-k+1}|^2)\mathcal{N}_{tot}(|\alpha\rangle)$, where $\chi_0=\chi_{2N+1}\equiv 0$. This result also means that

$$\mathcal{M}(j,k)=|\chi_{j-k}|^2+|\chi_{j-k+1}|^2. \tag{9}$$

Note that χ_r does not depend on the amplitude of the initial state but only on the structure of $\hat{U}_{QW}^N$.

The initial-state density operator in P representation can be generally written as [1,14]

$$\rho_0=\int d^2\alpha P(\alpha)|\alpha\rangle\langle\alpha|, \tag{10}$$

where $P(\alpha)$ is the P representation of the initial state ρ_0. Provided that $P(\alpha)$ is a sufficiently singular generalized function, such a representation exists for any given operator ρ_0 [14]. After N steps, the density operator evolves as

$$\rho_N=\hat{U}_{QW}^N\rho_0\hat{U}_{QW}^{N\dagger}=\int d^2\alpha P(\alpha)|\chi_1\alpha\rangle_1\langle\chi_1\alpha|\otimes\cdots\otimes|\chi_{2N}\alpha\rangle_{2N}\langle\chi_{2N}\alpha|, \tag{11}$$

where Eqs. (8) and (10) have been used. The P representation is particularly appropriate for our aim to find the average photon-number distribution since it can be shown that the moments of the P representation give the expectation values of normally ordered products of bosonic operators [1,14].

The marginal density matrix for mode r is simply obtained as

$$\rho_r=\int d^2\alpha P(\alpha)|\chi_r\alpha\rangle_r\langle\chi_r\alpha|. \tag{12}$$

The average photon number for the rth mode is

$$n_r=\mathrm{Tr}_r[\rho_r\hat{a}^\dagger\hat{a}]=|\chi_r|^2\int d^2\alpha P(\alpha)|\alpha|^2=|\chi_r|^2\mathcal{N}_{in}(\rho_0),$$

and the average photon number for the jth step and kth node is $\mathcal{N}_p(j,k)=\mathcal{M}(j,k)\mathcal{N}_{tot}(\rho_0)=(|\chi_{j-k}|^2+|\chi_{j-k+1}|^2)\mathcal{N}_{tot}(\rho_0)$, from which Eq. (9) is found to hold for the case of any input field. The interference pattern determined by $\mathcal{M}(j,k)$ does not depend on the initial input state. For a given set of beam splitters and phase shifters, any input state will result in the same interference pattern. Only an overall factor will be changed, according to the total average photon number of the initial state. For a classical light, in a pictorial way, the result is nothing but quantum random walks with many walkers simulated by interference between fields. For a weak field, the quantum random walks with a single walker can be probabilistically performed. For example, given a coherent state with $\alpha=1$, a single photon is detected with 37% of the probability.

A problem of the approach employing *dynamic lines* for quantum random walks is that the required number of resources (in terms of the number of optical elements required for a chosen number of steps and of the field modes involved) grows quadratically with the number of steps. This imposes serious limitations to the scalability of such a proposal and affects the efficiency of a simulation based on an interferometric device. In the alternative proposal in Fig. 3, this problem is bypassed measuring all the even positions by the upper row of detectors, while the odd ones are detected by the lower row. Acousto-optic modulators (AOMs) [12] are used to guide a beam toward a mirror for further steps or toward a detector for the measurement. When the AOMs in the top row have to deflect the light beams toward the detectors, those in the bottom row should not be active. The beam splitters and phase shifters in Figs. 1 and 3 are the same. The number of required resources, in this latter scheme, increases only linearly with the number of steps [19].

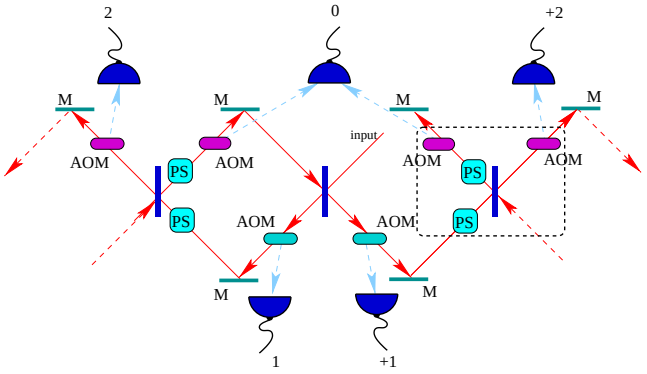

FIG. 3. Alternative setup for quantum random walk on a line. In this scheme, the number of required resources scales linearly with the number of steps N. Two rows of acousto-optic modulators (AOMs) direct the incoming beams of light to the perfect mirrors M or to the detectors row. This setup is conceptually equivalent to that sketched in Fig. 1(b).

There are many difficulties,for a practical implementation of the schemes we propose, that have to be taken into consideration. For example, being a multimode interferometric apparatus, the proposed setup could be affected by the misalignment of the involved optical elements. Furthermore, we need $2N$ modes for N steps of the walk process, which makes the controllability of the system very difficult. Nevertheless, even if these problems render the proposed setup challenging under an experimental point of view, our proposal has to be seen as a thought experiment useful for the investigation of the physics that is behind the appearance of the characteristic probability pattern of a quantum random walk.

IV. SIMULATION OF DECOHERENCE IN QUANTUM RANDOM WALKS

To better understand how interference effects are at the basis of a quantum walk process we study the effect that a certain class of errors has on the performance of the setup we propose. A decoherence mechanism is potentially able to wash out the interference pattern, thus erasing the speedup characteristic of a quantum walk and restoring some aspects of the classical diffusion process. In this section we study two different models for decoherence in our setup. We show the transition of the dynamics of the walker from the pure

quantum to the classical case. This analysis is in part motivated by the attention that has been recently paid to the way in which the quantum walk pattern is modified by imperfect coin tossings or walker translations, both for quantum walk on a line and higher dimensions [6,10]. A remarkable result, shown by Kendon and Tregenna in Ref. [10], is that small amounts of decoherence, rather than rendering the process useless for the purposes of quantum information, amazingly increase the capability of the system to explore its possible configurations. This gives a probability distribution to find the walker in a certain position that spreads faster than in pure dynamics. Our study is able to highlight even this aspect of the dynamics of the walker. On the other hand, studying the effects of possible sources of decoherence is worth from a practical point of view. The characterization of some relevant sources of errors, in the proposed setup, will make us understand why the pattern resulting from a performed experiment devoted to the realization of a quantum walk process could deviate from the ideality.

We have considered ulterior phase-shift operations performed just before and after each $\hat{T}_2$ transformation. The shift in these additional operations is randomly chosen from a Gaussian distribution. In what follows, we show how the mean-photon-number distribution changes its shape (from a classical Gaussian pattern to an approximately flat distribution then to a quantum distribution) as the amount of randomness in the additional phase shifts is reduced.

If l is a number randomly taken from a Gaussian distribution centered at 1 with an adjustable standard deviation σ_{pp}, we shift the phase of each field mode in Fig. 1(b) by an amount equal to $2\pi|l|$. If the phase shift is equal to 2π, the additional phase shifters are ineffective and a quantum walk pattern is recovered. On the other hand, if the amount of shifts deviates from this *neutral* value, they affect the interferences responsible for the quantum walk and some deviations have to be expected and the average over alarge number of trials results in a classical distribution.

In Fig. 4, the shown distributions are the results of an average over 50 different trials: in each one of them, and for each step in a single trial, a different random value for l is considered and the mean photon-number at the various locations on the final dynamic line is calculated, averaging over the outcome for each trial.

If, now, σ_{pp} is reduced (in Fig. 4, $\sigma_{pp}=0.0125$), the phase shifts vary over a small range of values around 2π. The dynamic evolution of the system is affected in such a way that no classical signature is evident in the mean-photon-number distribution. A highly nonclassical pattern is found and some deviations from the pure quantum random walk case are evident. The distribution is relatively flat over a region that is wider than the pure quantum case. This result is in good agreement with the analysis performed in Ref. [10] for a small amount of decoherence. In our case, the limited randomness imposed to the evolution of the photonic walker simulates the effect of a decoherent coin tossing. The remarkable feature in this analysis is that we have used just classical resources (linear optics elements and input coherent states). Nonetheless, we still simulate the relevant features of the transition from a pure quantum evolution to the classical

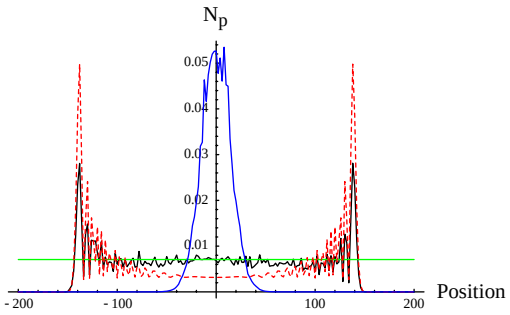

FIG. 4. Average photon-number distribution vs position for an input coherent state $|\alpha=1\rangle$ and for 200 steps. Different cases are considered: the bell-like curve represents the case of an introduced randomness l taken from a Gaussian distribution centered at 1 and with $\sigma_{pp}=0.25$. The curve evidently resembles the expected Gaussian distribution. The solid line shows the results for $\sigma_{pp}=0.0125$. It is compared with a uniform distribution between $-200/\sqrt{2}$ and $200/\sqrt{2}$, fictitiously extended to improve visibility. Finally, the dashed curve represents the pure quantum case corresponding to l chosen from a Dirac delta function $\delta(l-1)$. Each point in the simulated curves is averaged over 50 different trials.

spread due to a large superimposed randomness.

In Ref. [15], the effect of phase randomness in a general interferometric device has been investigated. In particular, if the device can be thought as the iterative applications of some basic units, each one affected by a fixed randomness [15], then Anderson localization can be obtained. Indeed, when fixed randomness is considered, a connection to the theory of the band-diagonal transfer matrix (examined in Ref. [16]) can be established. It is this kind of dynamic evolution that leads to localization of the walker. Physically, the model described in this case is near to the repeated passages of a beam of light through a dielectric layer placed inside an electromagnetic cavity, as described in Ref. [17]. In our model, however, no localization effect is achieved since different values for the phase shifts at each step are taken. In this respect, our case is far from a band-diagonal evolution. These qualitative arguments are resumed in Fig. 5, where the transition from a flat distribution (obtained for a small decoherence parameter σ_{pp}) to the classical one (relative to a strongly randomized quantum walk) is reported. To compare our results to those in Ref. [15] and to show that no dynamic localization is achieved here, we present plots for the average photon-number distributions in lin-log and in lin-lin scale.

Following the same lines depicted above, we can investigate about errors due to the uncertainty in the beam splitters transmittivities. We consider imperfect beam splitters whose transmittivities randomly fluctuate around 50% according to a Gaussian distribution with standard deviation σ_{bs}. Computing the normalized average photon-number distribution for an input coherent state, we find a narrow range of values for σ_{bs} within which a flat distribution is achieved. Outside this range, the distribution rapidly converges toward a classical one.

To give a picture of the combined effect of the two decoherence processes, we include random phase-shifters between two subsequent $\hat{T}_2$ operations and random fluctuations

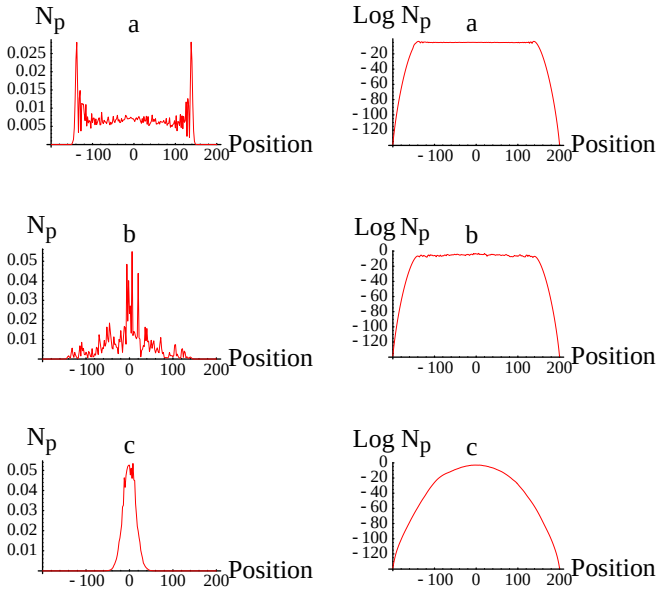

FIG. 5. Transition from weak to strong randomization in the model for decoherence in the coin tossing for an input coherent state $|\alpha=1\rangle$. From top to bottom, σ_{pp} is increased. We have considered $\sigma_{pp}=0.013$ (a), $\sigma_{pp}=0.13$ (b), and $\sigma_{pp}=0.25$ (c). The figures on the right show the same distributions presented in the left but in lin-log scale, with which the investigation of the appearance of localization effects is easier. The mean-photon-number distribution smoothly changes from a sharp-squared distribution to a concave curve that is typical of a classical distribution [15].

in the transmittivity of the beam splitters. In Fig. 6 we show the distribution that corresponds to $\sigma_{pp}=0.005$ and $\sigma_{bs}=0.07$. We can see that the mean-photondistribution has been very much flattened. Of course, as σ_{pp} and σ_{bs} grow, the curve will become Gaussian.

V. REMARKS AND DISCUSSION

As we discussed, the realization of the model we propose is not trivial as we pay the price represented by the use of $2N$

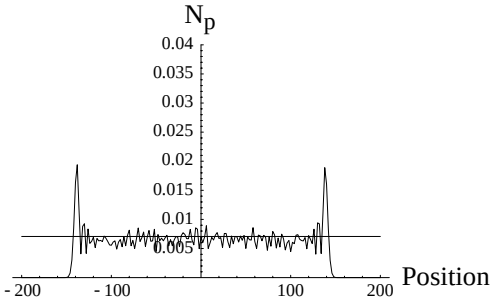

FIG. 6. Average photon-number distribution for an input state $|\alpha=1\rangle$ considering both the models of decoherence. The number of steps considered is 200 and each point is averaged over 50 different trials. We have taken $\sigma_{pp}=0.005$. On the other hand, we have taken $\theta=(\pi/2)|m|$ in $\hat{T}_2$, with a random number m extracted from a Gaussian distribution centered at 1 and having standard deviation $\sigma_{bs}=0.07$.

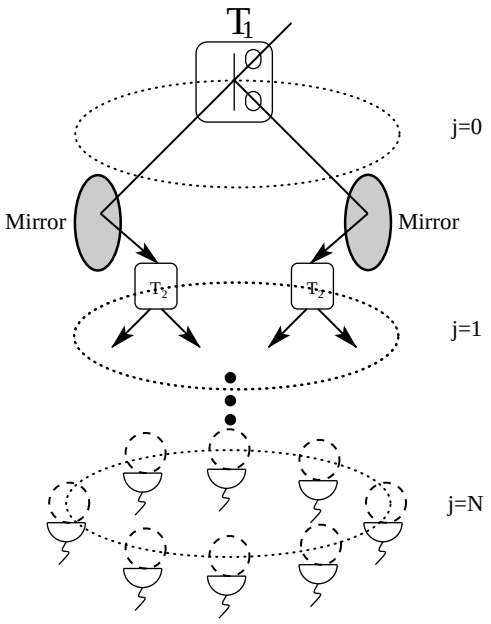

FIG. 7. An implementation of a quantum random walk on a circle using *dynamic circles.*

field modes to replace the quantum walker (that belongs to a Hilbert space of dimension N). Thus, the addition of a component, in our setup, increases the difficulty of alignment. However, what we want to stress in this paper is the possibility of simulating quantum random walks using the wave nature of a classical field. We have shown that this study has been possible using our thought experimental setup. Even though the results could be surprising, the possibility of such a simulation may be a natural result if we consider that quantum coherence and quantum interference are concepts originally borrowed from wave mechanics. This possibility has been formally proved using standard tools of quantum optics.

Furthermore, we have simulated some decoherence mechanisms on the quantum random walk by means of linear optical devices and input coherent states. We have observed how the average photon-number distributions are modified when controlled randomness is introduced in the system via additional phase shifters and imperfect beamsplitters. This analysis is useful both theoretically (clarifying the role of the coherent effects in the simulation) and practically because it characterizes the influences of possible sources of errors affecting the results of a performed experiment.

Finally, we want to mention here that it is in principle possible to extend our scheme to quantum random walks on a circle of N points, as shown schematically in Fig. 7. One can adapt the concept of dynamic line to that of *dynamic circles*: the walker transits from circle to circle (each having a nondecreasing number of sites on it) in a way completely similar to that described in Sec. II. The number of required dynamic circles is equal to N. Each site on a given circle is occupied by a basic operation: $\hat{T}_1$ occupies the unique site on the first dynamic circle, all the other sites in the following circles (labeled as $j=1,\ldots,N$ in Fig. 7) being occupied by $\hat{T}_2$. After each $\hat{T}_2$ operation, the beams are directed, by means of some mirrors, toward the proper site on the next

dynamic circle, as shown in Fig. 7 for the transition from the $j=0$ to the $j=1$ circle. At the final dynamic circle, the mean-photon-number distribution at the sites is revealed by an array of detectors. Basically, this implementation is still based on the simulation of a quantum walk on a line and it is, thus, obvious that it will simulate quantum walks on a circle with classical fields.

Under certain circumstances, our approach can be useful in order to simulate quantum walks on a hypercube of dimension 3. This higher-dimensional quantum walk can, indeed, be reduced to a biased quantum walk on a line with properly chosen, asymmetrical, probabilities for the coin to be in the $|R\rangle$ or in the $|L\rangle$ state [5]. As we have seen in Sec. II, properly choosing the parameters of the optical elements in $\hat{T}_1$, $\hat{T}_2$, our proposal is able to realize a quantum random walk on a line with any biased coin. We, thus, expect the possibility to simulate quantum walks on a three-dimensional hypercube by means of interference of classical light. However, the extension of these results to general graphs and hypercubes of higher dimensions (as well as an analysis of the efficiency of such a simulation) is much more difficult and goes beyond the purposes of this work. It is, however, worth stressing that the possibility of classical simulations of quantum random walk on a line does not necessarily imply its usefulness for a practical quantum algorithm. There remain important open questions about the gain, in terms of speedup of quantum computation, that can be obtained from the classical simulation of quantum walks.

Note added. Knight *et al*. also pointed out the possibility of simulation of quantum random walks using classical fields but using a totally different setup [18].

ACKNOWLEDGMENTS

We thank V. Kendon, G. M. Palma, I. A. Walmsley and Z. Zhao for stimulating discussions and useful comments. This work was supported by the UK Engineering and Physical Science Research Council Grant No. GR/S14023/01. M.P. acknowledges IRCEP for financial support.

[1] L. Mandel and E. Wolf, *Optical Coherence and Quantum Optics* (Cambridge University Press, Cambridge, 1995).

[2] U. Schöning, Proceedings of the 40th Annual Symposium on Foundations of Computer Science, New York, 1999 (unpublished); M. Jerrum, A. Sinclair, and E. Vigoda, Proceedings of the 33rd ACM Symposium on Theory of Computing, 2001 (unpublished).

[3] R. A. Dana and M. Jeanblanc, *Financial Markets in Continuous Time* (Springer, Berlin, 2002).

[4] A. Ambainis, E. Bach, A. Nayak, A. Vishwanath, and J. Watrous, in *Proceedings of the 33rd STOC* (Association for Comp. Machinery, New York, 2001); D. Aharanov, A. Ambainis, J. Kempe, U. Vazirani, *ibid.*; J. Kempe, e-print quant-ph/0205083.

[5] J. Kempe, Contemp. Physics **44**, 307 (2003).

[6] B.C. Travaglione and G.J. Milburn, Phys. Rev. A **65**, 032310 (2002); W. Dür, R. Raussendorf, V.M. Kendon, and H.-J. Briegel, *ibid.* **66**, 052319 (2002); B.C. Sanders, S.D. Bartlett, B. Tregenna, and P.L. Knight, *ibid.* **67**, 042305 (2003).

[7] Z. Zhao, J. Du, H. Li, T. Yang, Z.-B. Chen, and J.-W. Pan, e-print quant-ph/0212149.

[8] M. Hillery, J. Bergou, and E. Feldman, Phys. Rev. A **68**, 032314 (2003).

[9] A.M. Childs, E. Deotto, E. Farhi, J. Goldstone, S. Gutmann, and A.J. Landahl, Phys. Rev. A **66**, 032314 (2002); N. Shenvi, J. Kempe, and K.B. Whaley, quant-ph/0210064.

[10] V. Kendon and B. Tregenna, Phys. Rev. A **67**, 042315 (2003); T.A. Brun, H.A. Cateret, and A. Ambainis, *ibid.***67**, 032304 (2003).

[11] Note that classical random walks can be easily obtained by removing all the phase shifters. In this case, indeed, there can be no destructive interference that makes the quantum random walk different from its classical counterpart.

[12] A. Stefanov, H. Zbinden, N. Gisin, and A. Suarez, Phys. Rev. Lett. **88**, 120404 (2002).

[13] M.S. Kim, W. Son, V. Buzek, and P.L. Knight, Phys. Rev. A **65**, 032323 (2002).

[14] M. O. Scully and M. S. Zubairy, *Quantum Optics* (Cambridge University Press, Cambridge, 1997).

[15] P. Törmä, I. Jex, and W.P. Schleich, Phys. Rev. A **65**, 052110 (2002).

[16] F. Haake, *Quantum Signature of Chaos* (Springer-Verlag, Berlin, 1992).

[17] D. Bouwmeester, I. Marzoli, G. Karman, W.P. Schleich, and J.P. Woerdman, Phys. Rev. A **61**, 013410 (2000).

[18] P.L. Knight, E. Roldan, and J.E. Sipe, Phys. Rev. A **68**, 020301(R) (2003).

[19] More precisely, while the number of beam splitters grows as N, the required AOMs and phase shifters increases as $2N$. However, in the spirit of the proposal shown in Fig. 1, we can consider basic building blocks made by a beam splitter, two phase shifters, and two AOMs (as the one boxed in Fig. 3). This clarifies that, in this case, the number of building blocks grows linearly with N.